SOME NOTES ON LONG-PERIOD SIGNALS

Roy Greenfield

Ocean and Atmospheric Science, Incorporated

Prepared for:

Advanced Research Projects Agency
Air Force Office of Scientific Research

November 1974

UNCLASSIFIED

SECURITY CLASSIFICATION OF THIS PAGE (When Data Entered)

REPORT DOCUMENTATION PAGE		READ INSTRUCTIONS BEFORE COMPLETING FORM
1. REPORT NUMBER AFOSR - TR - 75 - 1899	2. GOVT ACCESSION NO.	3. RECIPIENT'S CATALOG NUMBER AD/A-004 825
4. TITLE (and Subtitle) SOME NOTES ON LONG-PERIOD SIGNALS		5. TYPE OF REPORT & PERIOD COVERED Quarterly: July 1, 1974 Sept. 30, 1974
		6. PERFORMING ORG. REPORT NUMBER TR 74-252
7. AUTHOR(s) Roy Greenfield		8. CONTRACT OR GRANT NUMBER(s) F44620-74-C-0066
9. PERFORMING ORGANIZATION NAME AND ADDRESS Ocean & Atmospheric Science, Inc. 145 Palisade Street, Dobbs Ferry, NY 10522		10. PROGRAM ELEMENT, PROJECT, TASK AREA & WORK UNIT NUMBERS 62701E AO 1827
11. CONTROLLING OFFICE NAME AND ADDRESS Advanced Research Projects Agency/NMR 1400 Wilson Boulevard, Arlington, VA 22209		12. REPORT DATE November [illegible], 1974
		13. NUMBER OF PAGES 43
14. MONITORING AGENCY NAME & ADDRESS(if different from Controlling Office) Air Force of Scientific Research/NP 1400 Wilson Boulevard Arlington, VA 22209		15. SECURITY CLASS. (of this report) UNCLASSIFIED
		15a. DECLASSIFICATION/DOWNGRADING SCHEDULE

16. DISTRIBUTION STATEMENT (of this Report)

Approved for public release; distribution unlimited

17. DISTRIBUTION STATEMENT (of the abstract entered in Block 20, if different from Report)

18. SUPPLEMENTARY NOTES

Nuclear seismic discrimination; surface wave; ellipticity constraint; mixed events.

19. KEY WORDS (Continue on reverse side if necessary and identify by block number)

Nuclear seismic discrimination; surface wave; ellipticity constraint; mixed events.

20. ABSTRACT (Continue on reverse side if necessary and identify by block number)

The problem investigated was the one of long-period signals (30-60 seconds) from a single three-component seismometer to determine the Love and Rayleigh components of an explosive event in the presence of noise or an interfering earthquake.

A review of current knowledge concerning long-period noise characteristics and interfering earthquake signals is made. In addition, a review of work concerning experimental studies of ellipticity is made. (OVER)

DD FORM 1 JAN 73 1473 EDITION OF 1 NOV 65 IS OBSOLETE

UNCLASSIFIED

SECURITY CLASSIFICATION OF THIS PAGE (When Data Entered)

20. Abstract (continued)

A critique of OAS's proposed ellipticity filter is made and some recommendations for improvement are given. These include the least-squares estimation of the explosion components assuming that the explosion azimuth is known.

OAS

OCEAN & ATMOSPHERIC SCIENCE, INC.
145 PALISADE STREET
DOBBS FERRY, NEW YORK 10522
914-693-9001

TR 74-252

SOME NOTES ON LONG-PERIOD SIGNALS

by

Dr. Roy Greenfield

Submitted under Contract No. F44620-74-C-0066

Submitted to:

Air Force Office of Scientific Research/NP
1400 Wilson Boulevard
Arlington, Virginia 22209

November 26, 1974

Form Approved
Budget Bureau No. 22-R0293

OAS

OCEAN & ATMOSPHERIC SCIENCE, INC.
145 PALISADE STREET
DOBBS FERRY, NEW YORK 10522
914-693-9001

QUARTERLY TECHNICAL REPORT NO. 2

For Period July 1, 1974 to September 30, 1974

Sponsored by
Advanced Research Projects Agency
ARPA Order No. 1827

ARPA Order Number:	1827
Program Code Number:	4F10
Name of Contractor:	Ocean & Atmospheric Science, Inc.
Effective Date of Contract:	April 1, 1974
Contract Expiration Date:	March 31, 1975
Amount of Contract Dollars:	$128,579
Contract Number:	F44620-74-C-0066
Principal Investigator and Phone Number:	Dr. Bernard Harris 914-693-9001
Program Manager and Phone Number:	Russell Gershman 914-693-9001
Short Title of Work:	Seismic Verification of Mixed Events

This research was supported by the Advanced Research Projects Agency of the Department of Defense and was monitored by the Air Force Office of Scientific Research under Contract No. F44620-74-C-0066

1C

TABLE OF CONTENTS

1.0 Assumptions

In this study I generally made the following assumptions and restrictions on what was considered:

1. We would have available only a single three-component seismometer;

2. We wish to find the frequency domain amplitude of both Love and Rayleigh waves of an explosive signal;

3. The origin time and great circle azimuth to the explosive source is known;

4. Interference may be natural or an interfering earthquake;

5. The period band of 20 to 60 seconds is of interest, with the primary interest in 40-second periods.

2.0 Literature

2.1 The Nature of Interference

A. The natural background (excludes identifiable interfering earthquakes):

1. At the shorter period end (20 to 30 seconds), the natural noise has two major components. Approximately half the noise power comes from propagating fundamental Rayleigh waves generated by ocean wave action. The level of this noise is variable with meteorological conditions in the oceans. The level of this component falls rapidly with increasing period from the peak at about 16 seconds. This portion of the noise is spacially coherent and usually comes from one or two major directions at any given time. The power level will be similar on horizontal and vertical instruments. The power level will not be decreased by seismometer burial (see Capon, 1969).

The remainder of the noise is locally generated by atmospheric loading. Turbulent loading is the most common method of generation, although occasionally an acoustic gravity wave will significantly add to the seismic noise. Seismometer burial decreases the noise level of the turbulent component, but not of the gravity wave noise. For shallow seismometers the horizontals will have a higher noise level than the verticals.

2. At the longer periods (30 to 60 seconds), the ocean generated microseisms are not significant. (Savino, et al., 1972b; Capon, 1969; Sorrells and Douse, 1974). The major noise source is from atmospheric turbulence static generation in the vicinity (approximately 500 m) of the seismometer. This noise has the following properties:

1. On the vertical seismometer, the minimum power level is at 30 to 40-second period;

2. The power level (at 30 seconds) is much higher (15 dB) on a surface seismometer compared to a deep one during turbulent atmospheric conditions, and about 3 dB higher during calm conditions. Power levels vary by about 15 dB with time;

3. Coherence between verticals is discussed by (Savino, et al, 1972b). The coherence is on the order of 0.59 for a 1 km separation;

4. (Savino, et al., 1972b, p. 189). There is no significant correlation between the horizontal component with the verticals over the period range of 10 to 500 seconds due to the noise being generated by many uncorrelated sources. (I believe that in the 10 to 30 second band there will at times be some coherence between horizontals and the vertical.);

5. Noise power levels for OGD are similar on horizontal and verticals (Savino, et al., 1972b)

B. Earthquake Interference

1. Major Arrivals

The initial, normally discussed, arrivals from earthquakes consist of the following. No effort is made to discuss these here since their properties are well known.

a. P and S body waves

b. Love waves (direct path)

c. Rayleigh waves (direct path)

d. major multibounce body waves, PP, SS, PPP, SSS, etc.

e. PL coupled leaky waves.

These arrivals are all arrivals occurring before the Rayleigh wave arrives.

2. Multipath Surface Waves

a. At 20 seconds

Many multipath arrivals are observed. Some multipath arrivals have power levels comparable to the main Rayleigh wave train. Azimuths of multipath arrivals and even the main Rayleigh wave may differ from the great circle path by as much as 40^{o}. The multipaths arise because of differences in phase velocity between different areas of the earth (especially between continents and oceans). These contrasts cause refraction of waves.

In addition, if a wave hits a boundary at a large angle to the normal, a significant amount of energy may be reflected. Thus, multipaths can arise even if source and receiver are on the same

continent. The best references for these multipaths are Capon(1970) and Capon and Evernden (1971). The interference of multipath arrivals is also noted by Newton (1973) and Boore and Toksöz (1969) (See Table I).

b. At 40 seconds

The properties of these multipath Rayleigh waves are very important for the present work. The most complete study of their properties is Capon and Evernden (1971). This work is based on pre-low-pass filtered data. Table 2 gives a compilation of their results. Note that the 6dB bandpass of the filter used after the prefilter was (.019 - .031 Hz) or (32 to 52 second period).

From this table it is observed that the highest power level is always in the first 200 second window, or in both the first and second windows. For the first window, the azimuth deviation (arrival angle difference from the great circle) is 0^{o} with the exception of a 10^{o} deviation for Event #17. Thus, an assumption, that the arrival direction of the main 40-second period wave is the great circle path, is justified.

The power levels of the later arriving multipaths is generally down 10dB and usually much more from the main arrival. The multipath arrivals do have angular deviations of an order of 20^{o} in some cases.

Table 1: Measured Variations in Azimuth of Arrival and Power Levels at Various Times for Events. From Capon (1970)

Event No	Time (sec)	Azimuthal Deviations*				Power Levels†			
		At 40 sec (deg)	At 33 sec (deg)	At 25 sec (deg)	At 20 sec (deg)	At 40 sec (db)	At 33 sec (db)	At 25 sec (db)	At 20 sec (db)
1	0-200	0	−5	−11	—	7	6	0	—
	200-400	—	11	11	−12	—	8	2	7
	400-600	—	—	11	10	—	—	5	4
	600-800	—	—	30	18	—	—	12	5
2	0-200	0	0	—	—	5	5	—	—
	200-400	—	0	—	—	—	2	—	—
	400-600	—	—	−5	−5	—	—	0	4
	600-800	—	—	−40	−12	—	—	7	2
3	0-200	0	−7	—	—	0	4	—	—
	200-400	—	0	−11	−10	—	3	9	12
	400-600	—	—	2	0	—	—	10	11
	600-800	—	—	17	10	—	—	23	17
4	0-200	0	0	—	−6	9	5	—	12
	200-400	—	0	0	—	—	4	0	—
	400-600	—	—	3	5	—	—	5	2
	600-800	—	—	—	16	—	—	—	4
5	0-200	0	0	—	—	5	0	—	—
	200-400	—	—	−8	−9	—	—	1	0
	400-600	—	—	−16	−13	—	—	9	8
	600-800	—	—	−20	−18	—	—	21	18
6	0-200	0	0	3	—	11	9	11	—
	200-400	—	13	3	3	—	8	5	13
	400-600	—	—	−6	3	—	—	1	0
	600-800	—	—	−55	−6	—	—	10	3
7	0-200	0	0	−5	—	10	9	0	—
	200-400	—	—	—	0	—	—	—	2
	400-600	—	—	24	—	—	—	16	—
	600-800	—	—	31	22	—	—	20	18
8	0-200	0	0	−3	—	3	2	0	—
	200-400	—	—	0	−5	—	—	8	4
	400-600	—	—	—	14	—	—	—	12
	600-800	—	—	—	—	—	—	—	—
9	0-200	0	0	−4	—	7	6	0	—
	200-400	—	—	−4	−6	—	—	10	5
	400-600	—	—	12	18	—	—	13	14
	600-800	—	—	30	18	—	—	18	17
10	0-200	3	3	—	—	20	19	—	—
	200-400	3	3	0	—	4	0	3	—
	400-600	—	—	−2	−3	—	—	2	3
	600-800	—	—	—	—	—	—	—	—
11	0-200	−5	−6	−25	—	13	12	10	—
	200-400	—	—	−5	−20	—	—	4	9
	400-600	—	—	8	−20	—	—	1	2
	600-800	—	—	—	−6	—	—	—	0
12	0-200	−8	−12	—	—	3	1	—	—
	200-400	—	8	−14	50	—	7	0	2
	400-600	−28	−28	−17	—	12	7	3	—
	600-800	—	−28	—	—	—	12	—	—
13	0-200	−3	−4	—	—	9	11	—	—
	200-400	—	0	2	—	—	6	0	—
	400-600	36	—	37	−5	14	—	5	5
	600-800	41	37	−25	34	15	13	10	14
14	0-200	0	−4	−7	—	11	7	11	—
	200-400	—	21	−7	−2	—	9	1	7
	400-600	—	29	0	−2	—	10	4	0
	600-800	—	—	39	−2	—	—	10	4

Table 1: (contd) Measured Variations in Azimuth of Arrival and Power Levels at Various Times for Events. From Capon (1970)

Event No.	Time (sec)	Azimuthal Deviations*				Power Levels†			
		At 40 sec (deg)	At 33 sec (deg)	At 25 sec (deg)	At 20 sec (deg)	At 40 sec (db)	At 33 sec (db)	At 25 sec (db)	At 20 sec (db)
15	0–200	0	−4	−9	—	14	8	0	—
	200–400	—	—	6	−10	—	—	6	1
	400–600	—	—	—	0	—	—	—	7
	600–800	—	—	26	26	—	—	14	10
16	0–200	0	0	0	—	4	2	7	—
	200–400	25	13	−5	−10	8	6	2	5
	400–600	25	13	7	−10	12	3	0	5
	600–800	25	25	25	−10	10	8	5	7
17	0–200	10	10	7	—	12	11	19	—
	200–400	—	10	7	5	—	11	7	8
	400–600	—	—	—	5	—	—	—	0
	600–800	—	—	—	−17	—	—	—	8
18	0–200	0	2	—	—	9	3	—	—
	200–400	—	—	2	3	—	—	0	0
	400–600	—	—	27	7	—	—	14	13
	600–800	—	—	37	—	—	—	17	—
19	0–200	0	0	—	—	6	0	—	—
	200–400	0	0	2	−6	5	8	7	11
	400–600	2	2	−6	−6	1	4	2	9
	600–800	—	—	−6	−8	—	—	1	5
20	0–200	0	0	—	—	7	20	—	—
	200–400	0	0	0	0	10	3	0	8
	400–600	—	—	0	0	—	—	9	0
	600–800	—	—	−31	−23	—	—	10	18
21	0–200	0	−5	−7	—	13	6	5	—
	200–400	—	—	−11	−9	—	—	3	0
	400–600	—	—	—	—	—	—	—	—
	600–800	—	—	—	—	—	—	—	—
22	0–200	0	0	3	—	9	6	13	—
	200–400	—	—	3	3	—	—	0	11
	400–600	—	—	—	10	—	—	—	4
	600–800	—	—	—	10	—	—	—	8
23	0–200	0	0	0	—	6	4	0	—
	200–400	—	—	−29	−29	—	—	7	1
	400–600	—	—	−39	−39	—	—	4	10
	600–800	—	—	−39	−39	—	—	13	14
24	0–200	0	0	7	13	7	5	0	4
	200–400	—	—	—	15	—	—	—	10
	400–600	—	—	—	—	—	—	—	—
	600–800	—	—	—	—	—	—	—	—
25	0–200	0	−5	—	—	5	0	—	—
	200–400	—	10	−12	−19	—	9	0	6
	400–600	—	—	3	3	—	—	5	2
	600–800	—	—	10	10	—	—	8	8
26	0–200	0	0	—	—	14	13	—	—
	200–400	—	0	0	6	—	10	2	0
	400–600	—	—	—	6	—	—	—	14
	600–800	—	—	—	—	—	—	—	—

† Power levels in db relative to maximum power.

* Azimuthal deviations are differences between measured azimuth of arrival and true azimuth of epicenter of event.

Table 2: Measured Variations in Azimuth of Arrival and Power Levels at Various Times of the 40-sec Period Rayleigh Wave Group for 10 Events. From Capon and Evernden (1971)

Event No.	Time* (sec)	Azimuthal Deviation† (Deg)	Power Level‡ (db)
1	0-200	0	0
	200-400	16	−13
	400-600	—§	−20
	600-800	—§	−18
	800-1000	—§	−19
	1000-1200	—§	−22
	1200-1400	—§	−20
	1400-1600	—§	−19
2	0-200	0	0
	200-400	0	−5
	400-600	0	−16
	600-800	—‖	−25
	800-1000	—‖	−24
	1000-1200	—‖	−23
	1200-1400	—‖	−17
	1400-1600	—‖	−21
3	0-200	0	0
	200-400	0	−1
	400-600	0	−24
	600-800	—§	−32
	800-1000	−30	−29
	1000-1200	−30	−27
	1200-1400	—§	−33
	1400-1600	—§	−31
6	0-200	0	0
	200-400	0	−9
	400-600	20	−9
	600-800	20	−8
	800-1000	20	−8
	1000-1200	—‖	−11
	1200-1400	—‖	−13
	1400-1600	—‖	−19
8	0-200	0	0
	200-400	0	−14
	400-600	—‖	−30
	600-800	—‖	−34
	800-1000	—‖	−30
	1000-1200	—‖	−36
	1200-1400	—‖	−38
	1400-1600	—‖	−40
16	0-200	0	0
	200-400	12	0
	400-600	—‖	−7
	600-800	25	−7
	800-1000	—‖	−7
	1000-1200	—§	−13
	1200-1400	—§	−11
	1400-1600	—‖	−8

] similar power in two windows

Table 2: (contd.) Measured Variations in Azimuth of Arrival and Power Levels at Various Times of the 40-sec Period Rayleigh Wave Group for 10 Events. From Capon and Evernden (1971)

Event No.	Time* (sec)	Azimuthal Deviation†, (Deg)	Power Level‡ (db)
17	0-200	10	0
	200-400	10	−6
	400-600	—‖	−16
	600-800	—‖	−17
	800-1000	—§	−18
	1000-1200	—§	−21
	1200-1400	—§	−23
	1400-1600	—§	−22
19	0-200	0	0]
	200-400	0	0]
	400-600	—‖	−15
	600-800	—‖	−20
	800-1000	−17	−21
	1000-1200	—‖	−24
	1200-1400	−122	−23
	1400-1600	−30	−22
22	0-200	0	0
	200-400	0	−10
	400-600	58	−22
	600-800	—‖	−22
	800-1000	—‖	−23
	1000-1200	—‖	−29
	1200-1400	—‖	−24
	1400-1600	—‖	−27
25	0-200	0	0
	200-400	19	−13
	400-600	—§	−19
	600-800	—§	−18
	800-1000	—§	−15
	1000-1200	—§	−18
	1200-1400	—§	−18
	1400-1600	—§	−16

* Time is measured relative to onset of Rayleigh wave.

† Azimuthal deviations are differences between measured azimuth of arrival and true azimuth of epicenter of event.

‡ Power levels in decibels relative to power of main group.

§ Power level is below that of background noise and no direction of arrival can be assigned.

‖ Power level is above that of background noise but no direction of arrival can be assigned.

The description of Love wave multipaths at 40 second period is given by Capon (1971, L). The Love wave multipaths have similar properties (azimuth deviations and relative power) as the Rayleigh wave multipaths.

3. Late Arriving Earthquake Interference

By late arriving interference, we mean energy which comes after the Rayleigh wave and "simple" multipaths. This interference includes

a) Surface waves going the long way around the earth or going around more than once,

b) Multibounce body waves,

c) PKPPKP (also called P'P') waves. We will be discussing the roughly 40 second and above period range.

Capon and Evernden (1971) - note that the coda level decays rapidly to more than 30 dB below the main Rayleigh arrival in 6-7 minutes for some events. For other events, the coda decreases much more slowly, with coda only 7 to 13 dB below the main Rayleigh wave power for period of 5,000 seconds or more. Rates of decay are shown in Figure 0, for the first 26 minutes.

By f-k determinations of azimuth and phase velocity across LASA,

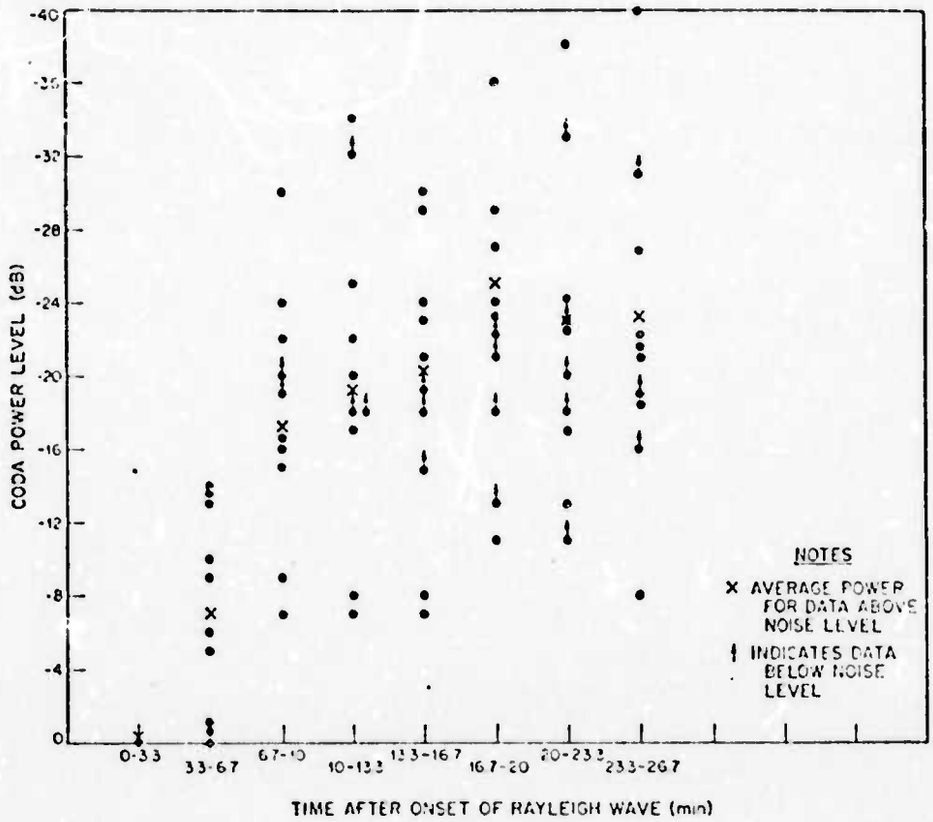

(a)

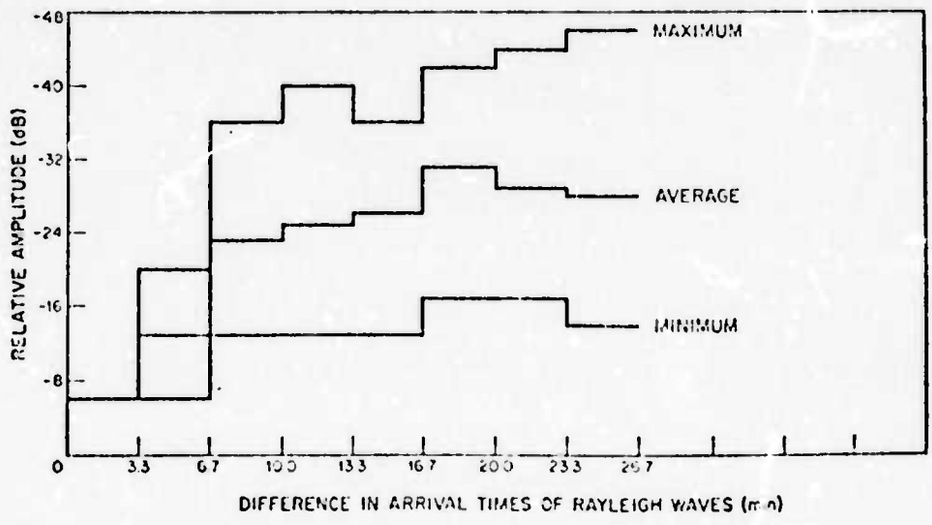

(b)

Fig. 0: Rate of Decay of Coda Power Level and Performance Characteristic of Proposed Detection Method. From Capon and Evernden (1971)

Capon and Evernden (1971) identified waves from the paths a), b), and c) described above.

Savino et al.(1972 b) p 168

They give the duration of coda from large events (average body wave magnitude of 6) as approximately 9 hours at Ogdensburg, (OGB), but note that the predominant periods are 60-180 seconds. Thus, much of this coda is out of our band. This type of coda dominates the OGB record approximately 10% of the time. I speculate that with a high pass cutoff at 60 second period, the fraction of time that the earthquake coda predominates the atmospheric noise would be greatly reduced.

Savino et al. (1974 b, p. 167)

Following Alsop and Brune (1965) it is suggested that multiply reflected P and S body waves make up a large portion of the late coda. This agrees with Capon and Evernden (1971). We note that the polarization (ellipticity) of body waves will be much different from Rayleigh waves. If the wave arrives at the seismometer as a P wave, it will be predominantly on the vertical; and if, as an S wave, predominantly on the horizontals. (I have not checked this last statement carefully for 40 second and longer waves, but I do know of some literature to look at if you desire) (Fig. 1 gives OGD seismograms from several events).

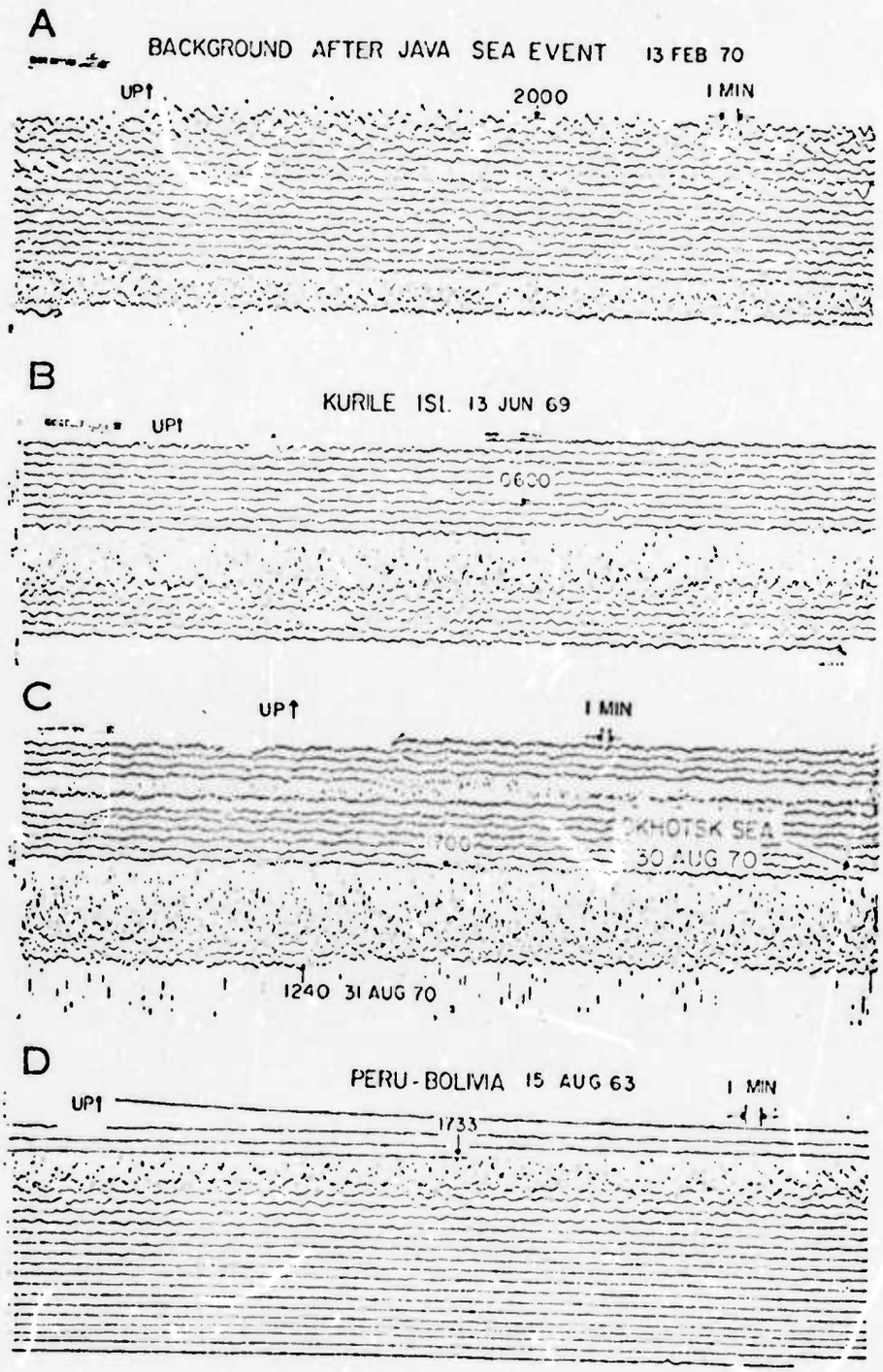

Fig. 1: Comparison of High-Gain Seismograms (A), (B), and (C) at OGD with a relatively low-gain Seismogram (D) from an instrument at Palisades, New York, for the duration of Intermediate and Deep-Focus Earthquakes. Epicentral Data for the Earthquakes in (A), (B), and (C) are given in Table 3. The Epicentral Data Reported by the USCGS for the Event in (D) are Aug. 15, 1963, 17h25m06s, 13.8S, 69.3W, Peru, Bolivia, h = 543 km. The magnitude was estimated at 7 1/4 by the Seismological Laboratory, Pasadena.
From Savino et al. 1972

The general duration of coda at 40-60 second period and its properties (i.e., types of waves) does not seem to have been published. Neither Savino et al. or Capon and Evernden have addressed the very late coda in this band systematically.

Savino et al. (1972 a)

They give results from 8 of the high gain stations. Detection ability is discussed, as is noise levels at the various stations. Band pass filtering is discussed as is polarization filtering.

2.2 Ellipticity Values and Variations

Boore and Toksöz

Phase difference between vertical and horizontal components were usually $90^{o} \pm 10^{o}$ (p. 339). This paper also shows theoretical phase between horizontal and verticals for multipath interference. Interference peaks are usually between 20 and 30 seconds.

Figure 2 shows ellipticity values and gives a means of estimating scatter as a function of period.

Newton

Figure 3 shows scatter of azimuth of arrival data. f-k analysis with LASA gives about $\pm$ 5% ('90%' confident'' limited to great circle azimuth. (See also Newton, p. c3). Using amplitude ratios of horizontal power of f-k gives errors in azimuth of about 8^{o} both positive and negative. This work was done, however, on only a few carefully selected earthquakes, and applied to the main part of the Rayleigh wave train.

Higher mode Rayleigh waves were also studied. These waves have higher group velocity than the fundamental mode and arrive somewhat before the fundamental mode. The ellipticity for these higher modes differs from the ellipticity of the fundamental mode. (Figure 4, a, b, and c)

On Figure 5, I have compared the Boore-Toksoz results with Newton. Note that they differ.

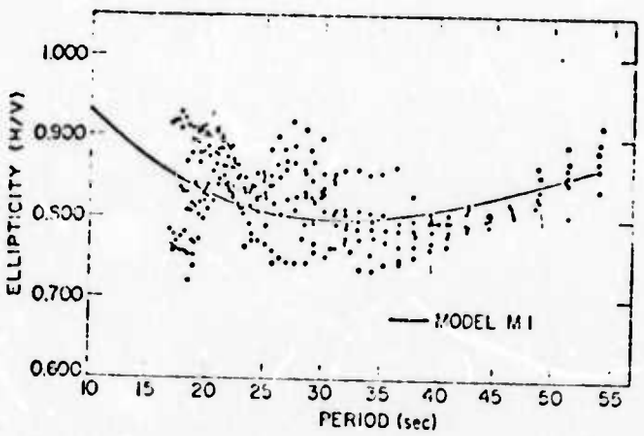

Fig. 2: Measured Ellipticity for Different Events and Different Sites. The Solid Line is the Theoretical Ellipticity Corresponding to Model M1. From Boore and Toksoz.

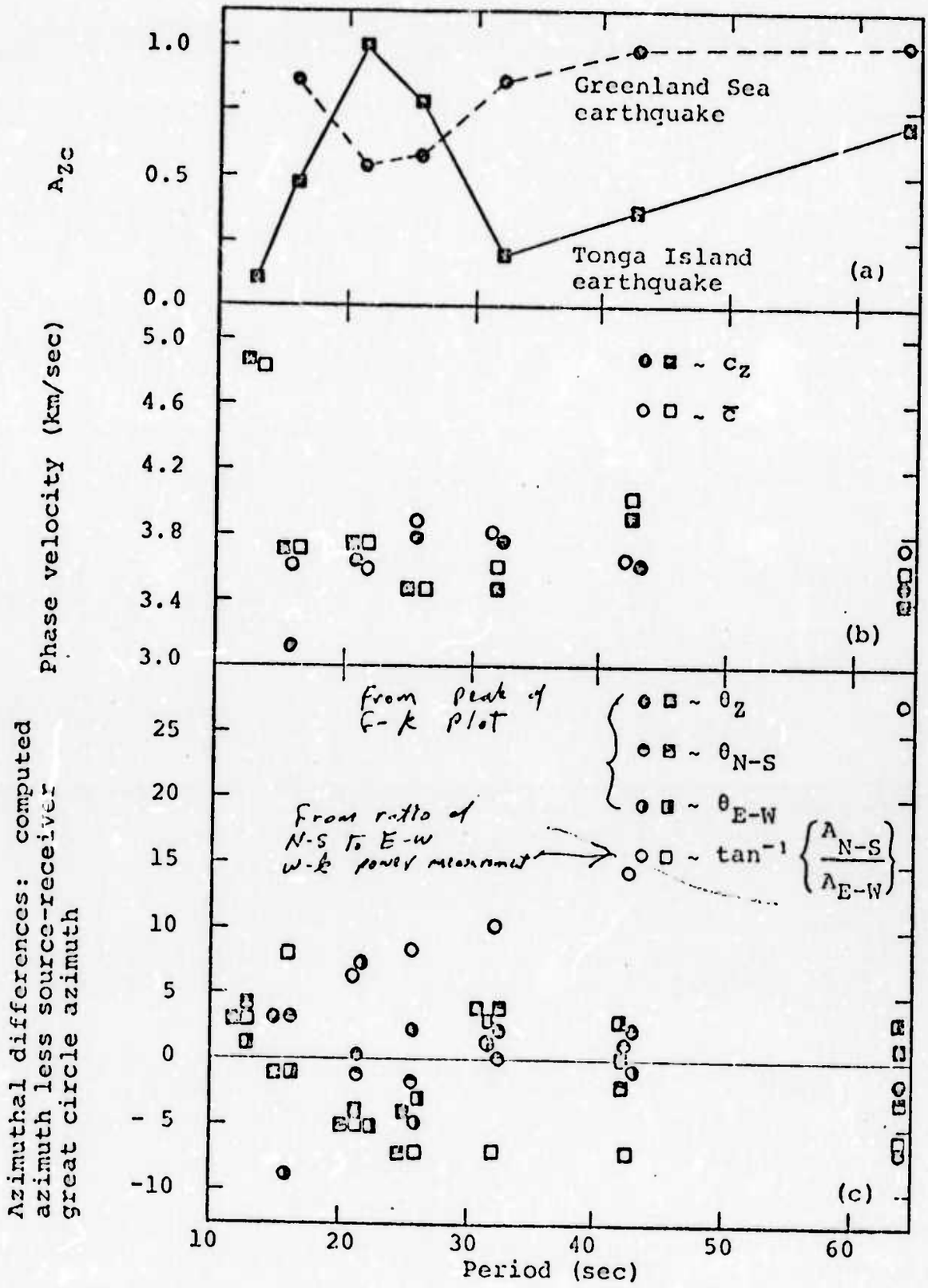

Fig. 3: Results of the f-k Analysis of Signals from the Tonga Island and Greenland Sea Earthquakes. (a) Normalized Amplitude Spectra. (b) Phase Velocities. (c) Propagation Directions. (From Newton, 1973, p. 109)

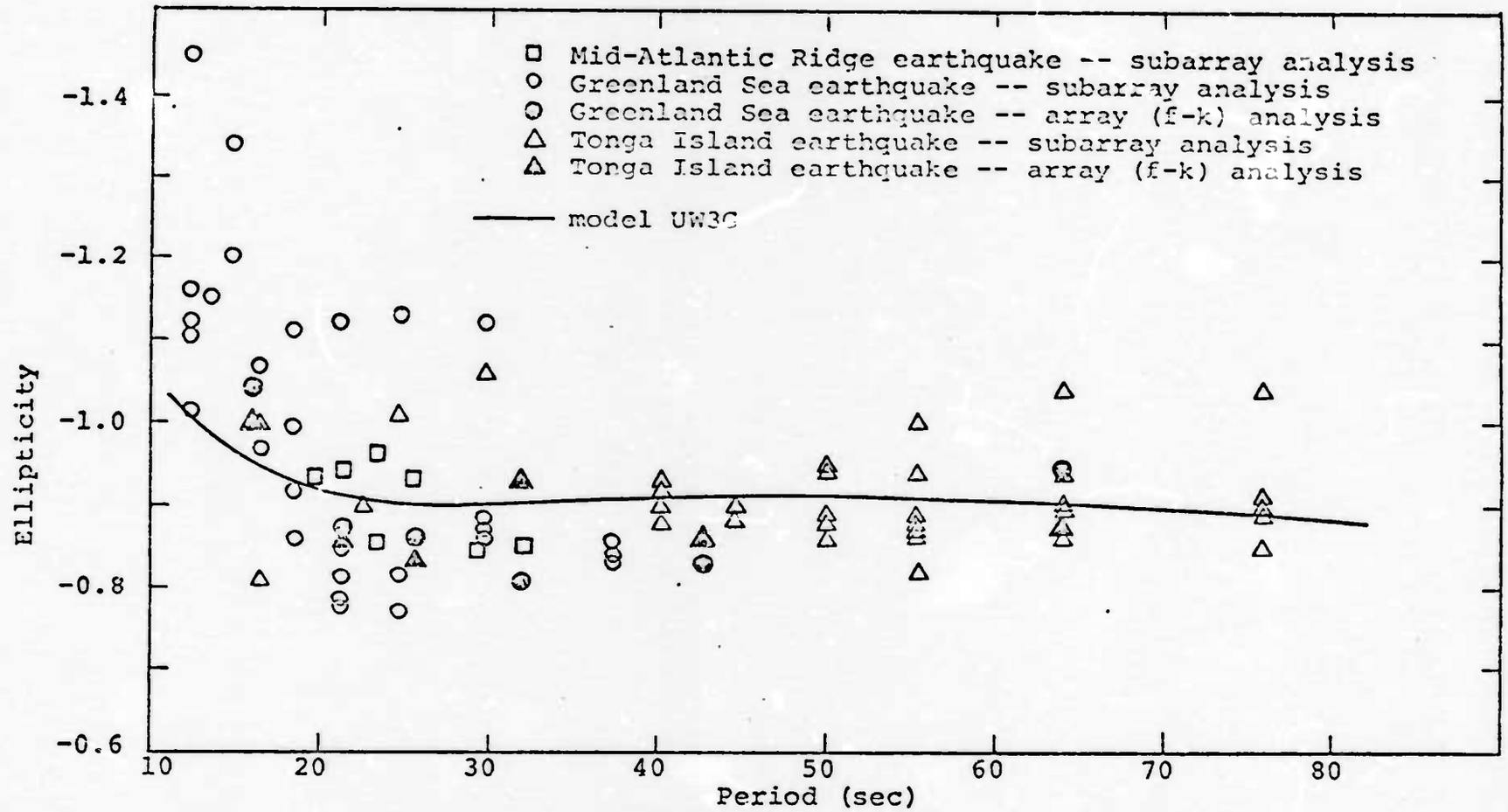

Fig. 4a: Composites of Ellipticities Observed at the LASA Subarrays in Group I. From Newton (1973)

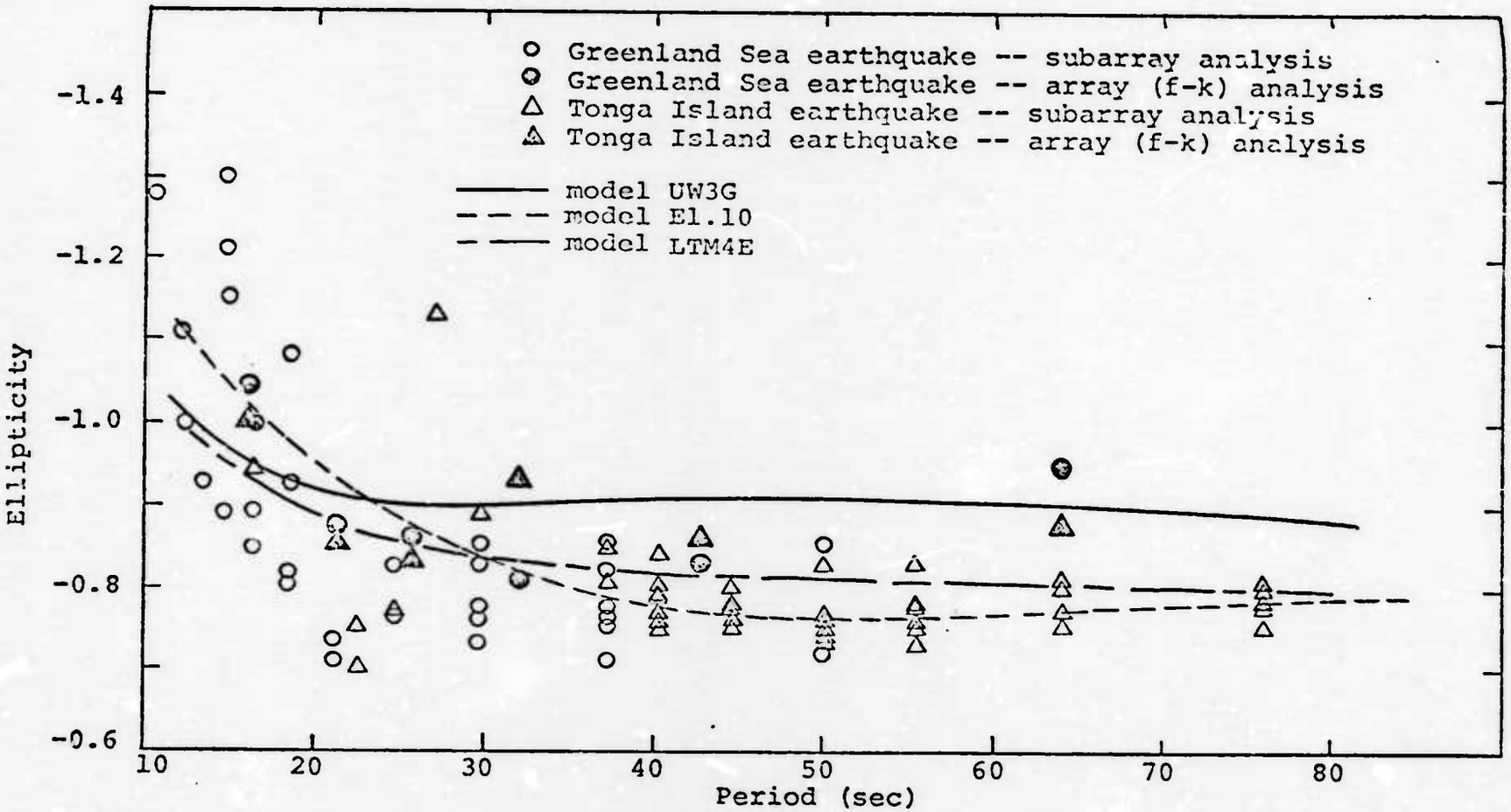

Fig. 4B: Composite of Ellipticities Observed at the LASA Subarray in Group II. From Newton(1973)

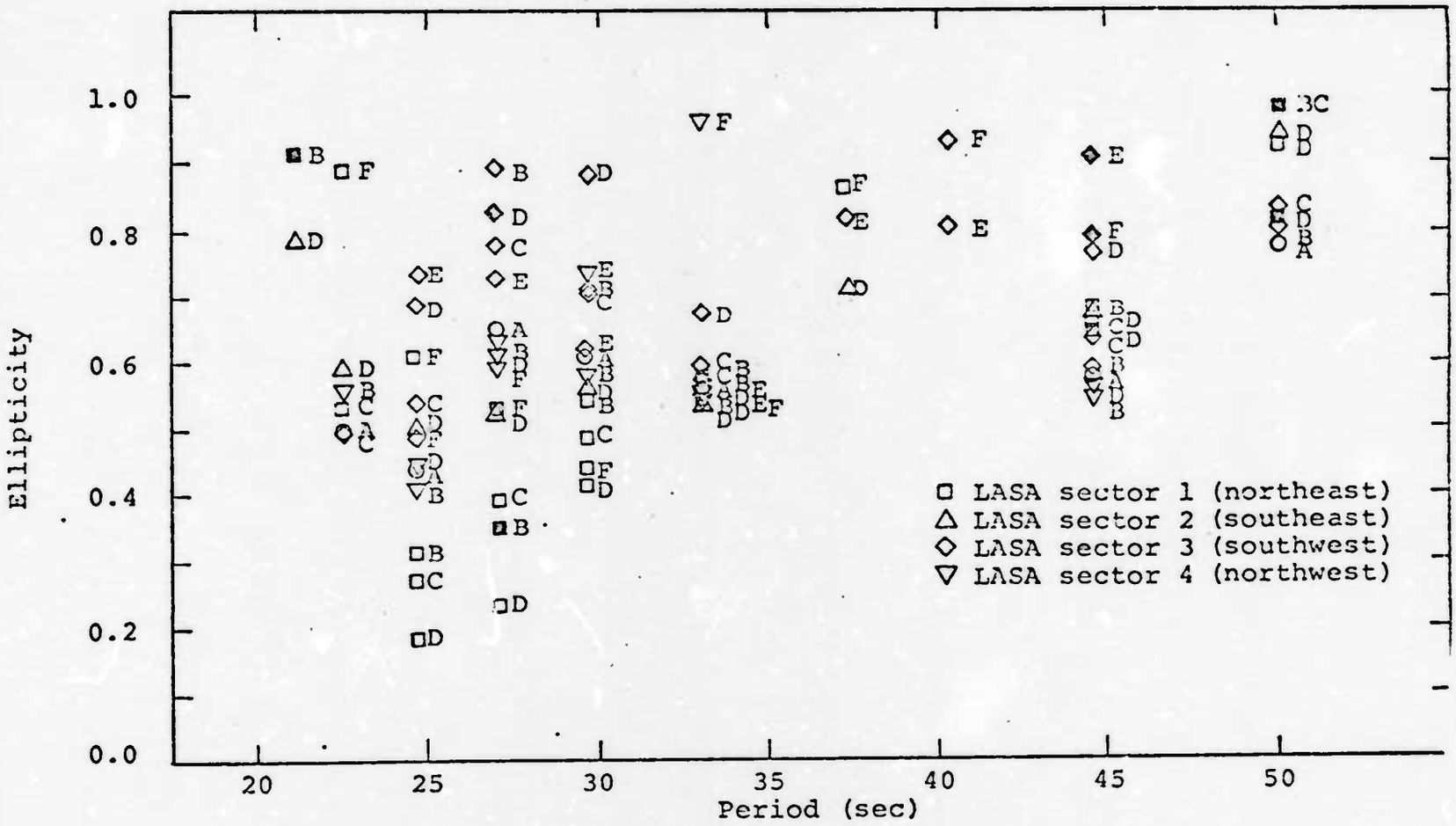

Fig. 4c: Higher Mode Ellipticities from Observations at LASA Subarrays of the Tonga Island Earthquake Signals. Open Symbols Denote Reciprocal Ellipticity (i.e., Vertical over Radial Spectral Amplitudes)
Note: These will usually arrive before the Fundamental.

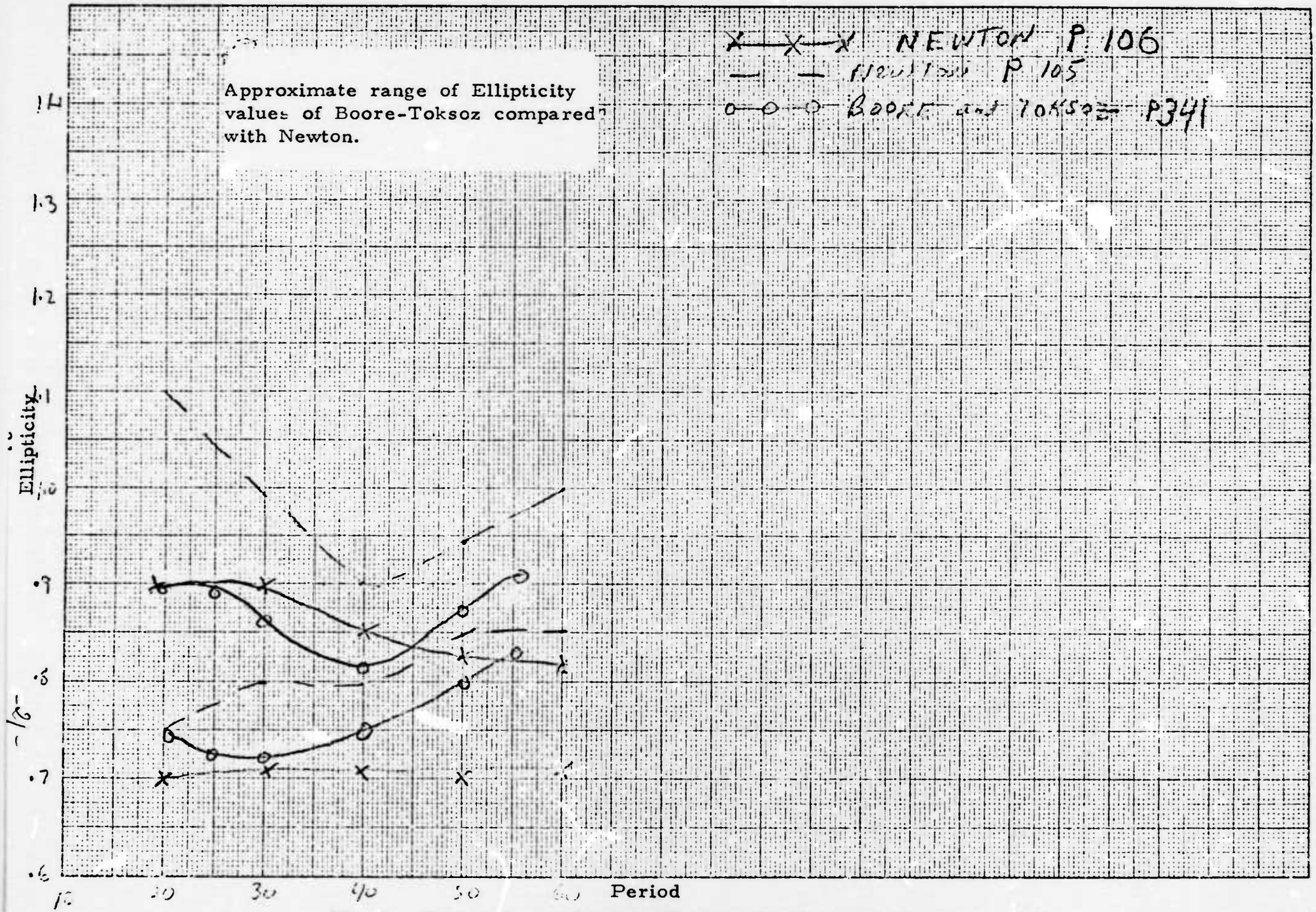

Fig. 5: Comparison of Boore-Toksoz Results with Newton Results

3.0 Critique of Present Approach

3.1 On Spectral Estimation Procedures

The direct part of the Rayleigh wave (excluding multipath arrivals) is in the frequency domain

$$e^{-i(\omega/c(\omega))r}$$

where $c(\omega)$ is phase velocity, $k = \omega/c$

r is range

and the arrival time of a given frequency is given by

$$t_a = r/U(\omega)$$

where $U(\omega)$ is the group velocity, given by $\delta k/\delta\omega$

For the 40 to 60 second period range $U(\omega)$ is fairly constant. Thus, energy arrives over a fairly short period of time. Figures 6 and 7 show LASA LPZ seismograms after filtering by the filter shown in Figure 8. For the event of Figure 6, the energy is contained in a 200 second window. Thus, a 200 second window, as presently being used by OAS, is sufficient for this event. However, it remains to develop a method to select the proper time interval.

Overlapping windows, starting every 30 seconds would probably assure one window covered the arrival. Perhaps, the criteria of the window with the most energy in the explosive event

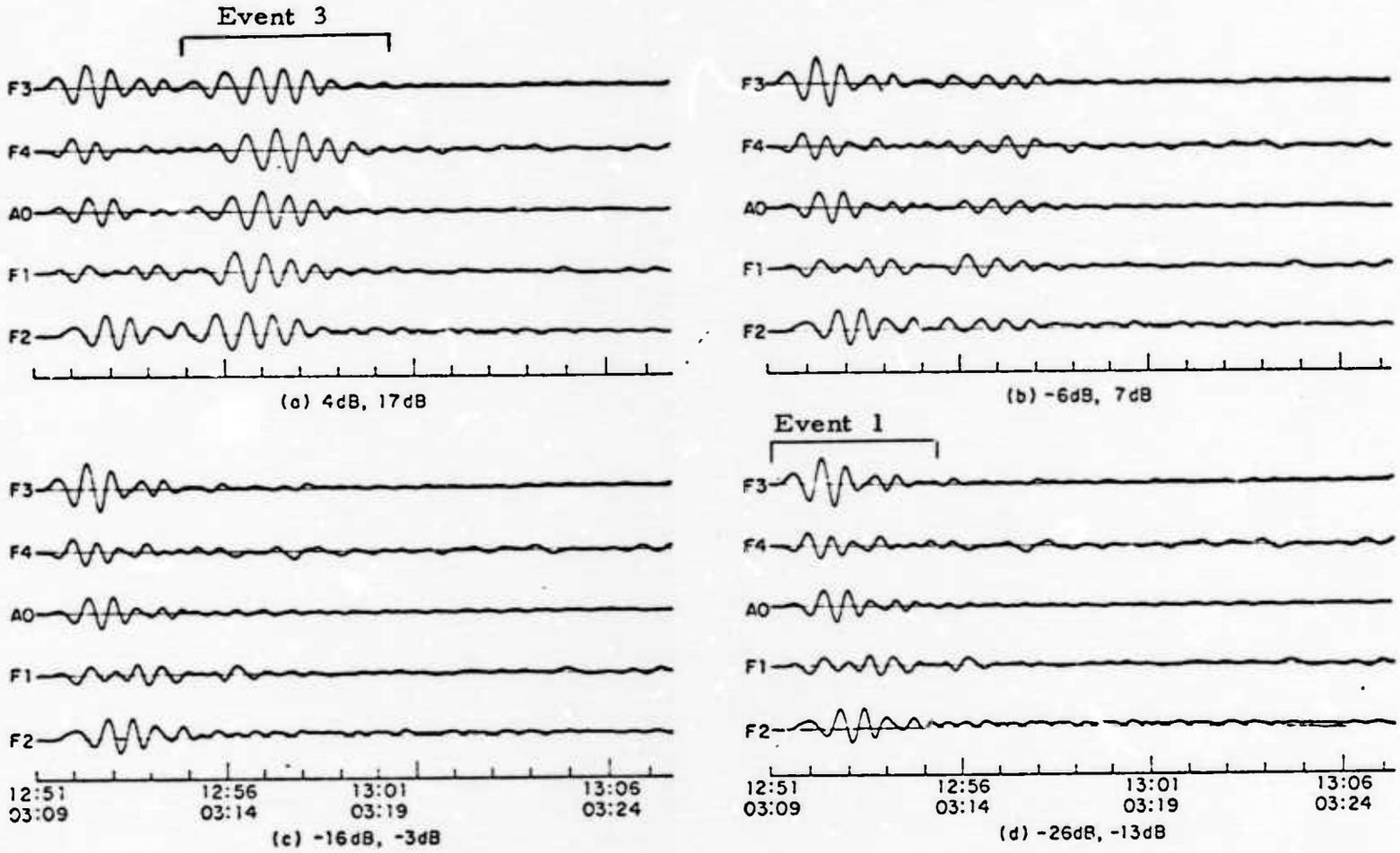

Fig. 6: The Prefiltered Wave Forms for Event 1 Added Artifically to Those of Event 3. From Capon and Evernden (1971)

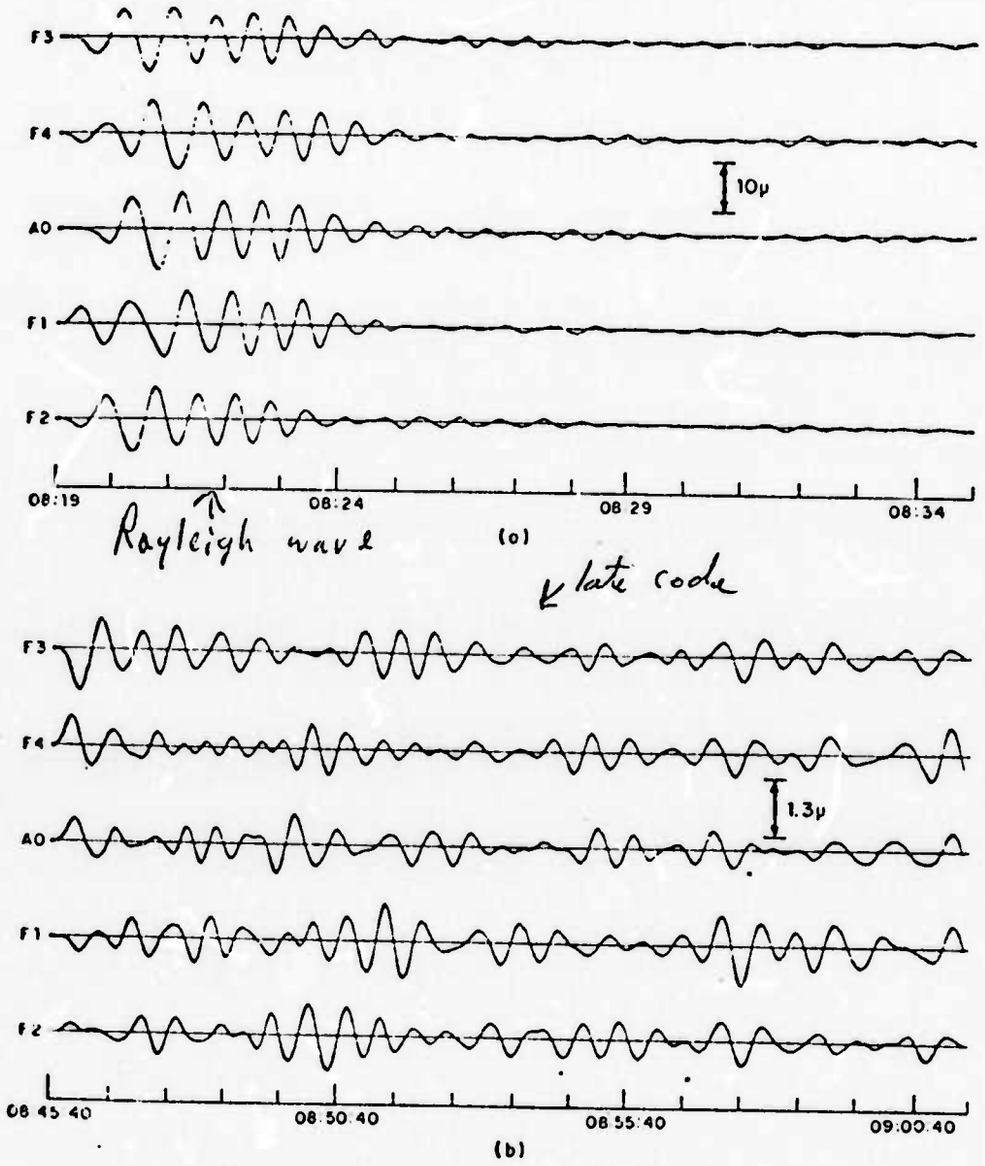

Note:
Gain
Change

Fig. 7: Prefiltered Wave Forms of Event 19 of October 15, 1967, near the Coast of Nicaragua, Showing Initial Rayleigh-Wave Group Arrival and Multiply Reflected P Waves. From Capon and Evernden (1971)

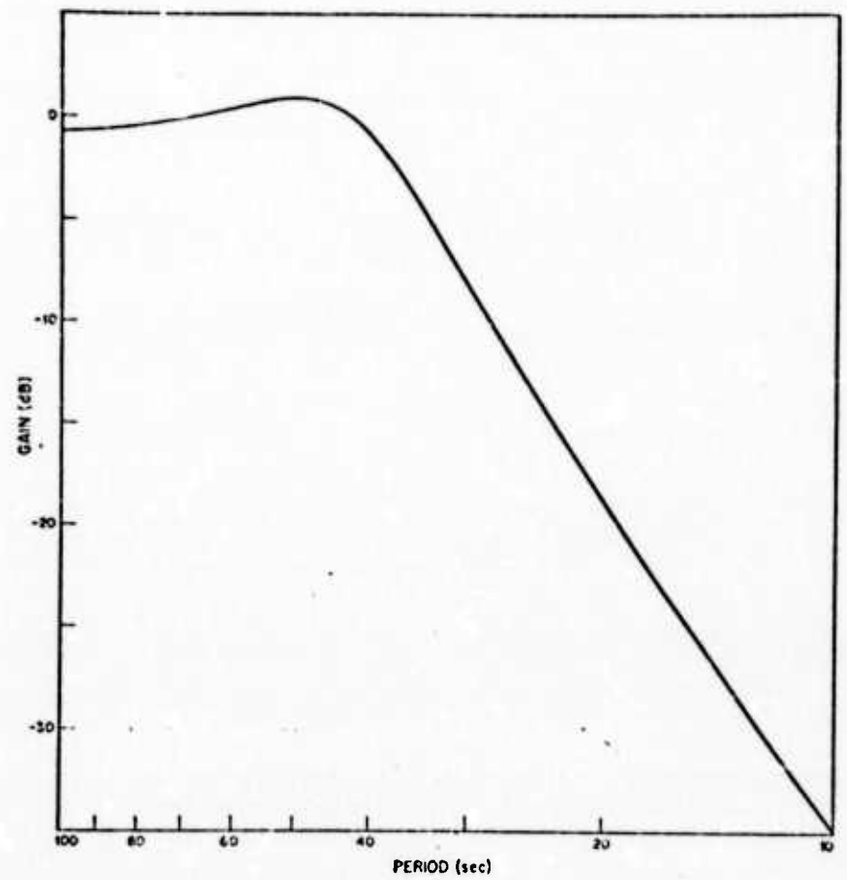

(a)

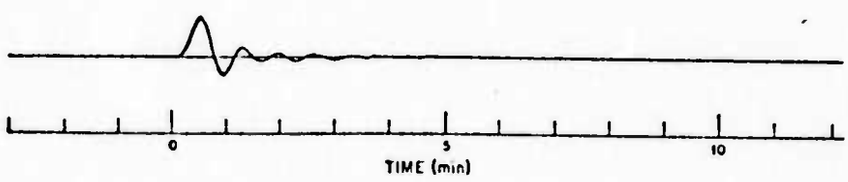

(b)

Fig. 8: Frequency Response and Impulse Response of of Fifth Order Low-Pass Chebyshev Filter. From Capon and Evernden (1971) Pre Low-Pass Filter.

azimuth direction (on the rotated horizontal) could be used to determine which of the windows actually contains the arrival.

If the window used does not contain most of the energy in the arrival, I would expect an error in the measured phase spectrum. Figure 7 shows an event (#19) with a Rayleigh wave of 300 seconds length. From Table 2, we see that, for three (Events 3, 16, and 19) of the ten studied, the power levels were similar for the first two 200 second windows. For these events, a longer window should be used.

For the 20-40 second band, the group velocity increases with period. This portion of the Rayleigh wave train is highly dispersed and typically arrives over a 400-600 second period (the arrivals are extended even more in time by multipaths). Thus, for this period range no single 200 second window will contain all frequencies. Results of Capon and Evernden (1971, p. 819) and Newton (1973) demonstrate this point. Also see Table I and records shown in Figures 9-14.

I have not presently developed this approach, but rather than using spectral analysis, the bank of bandpass filters approach with cross correlations between components to separate the Rayleigh waves of two events might be considered.

For the LASA (25 second Peak) seismometers, 20 second period energy leaked through the digital filters into the 40 second

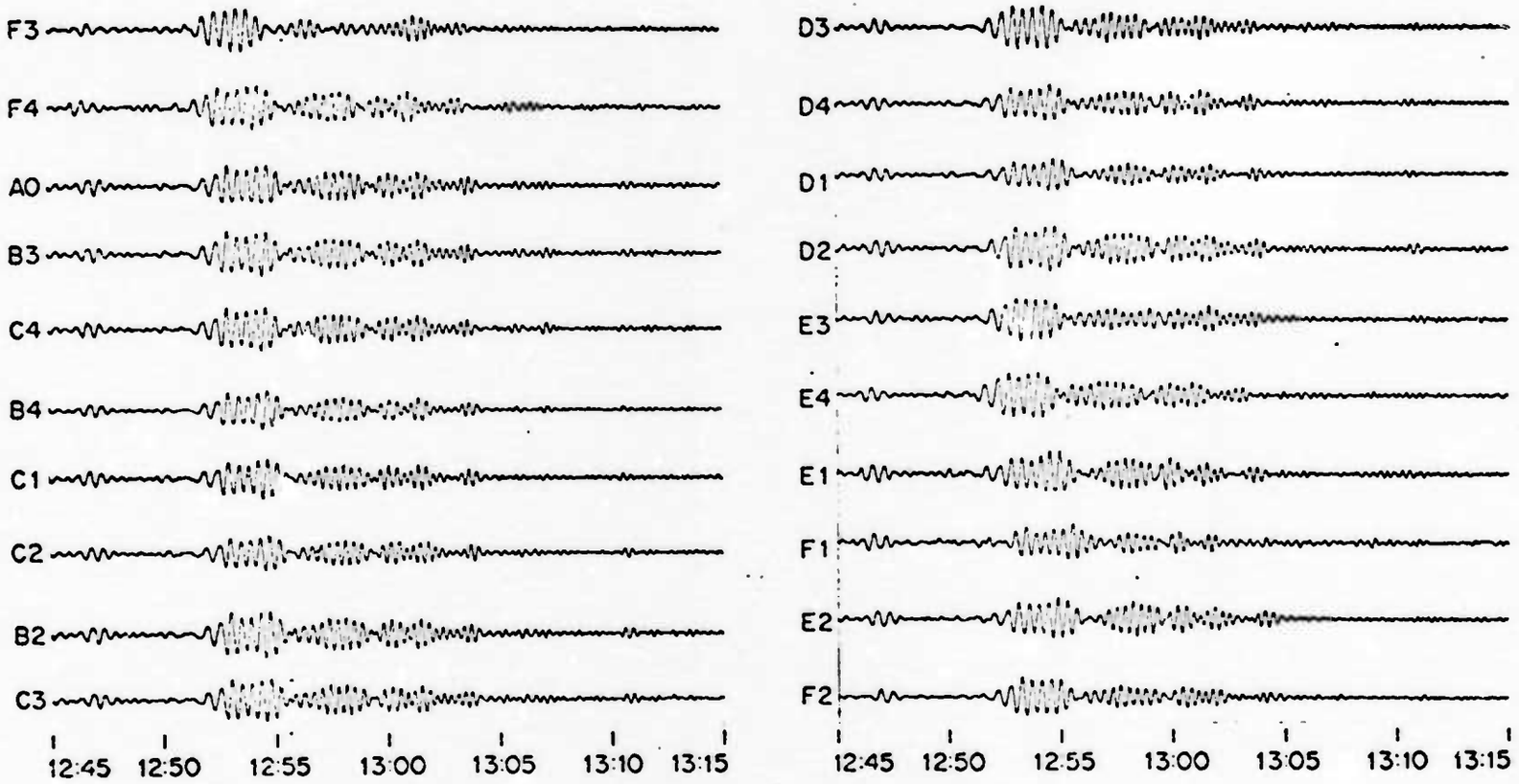

Fig. 9: The Long-Period Wave Forms for Event 1, the November 21, 1966, Kurile Islands Event. From Capon and Evernden (1971)

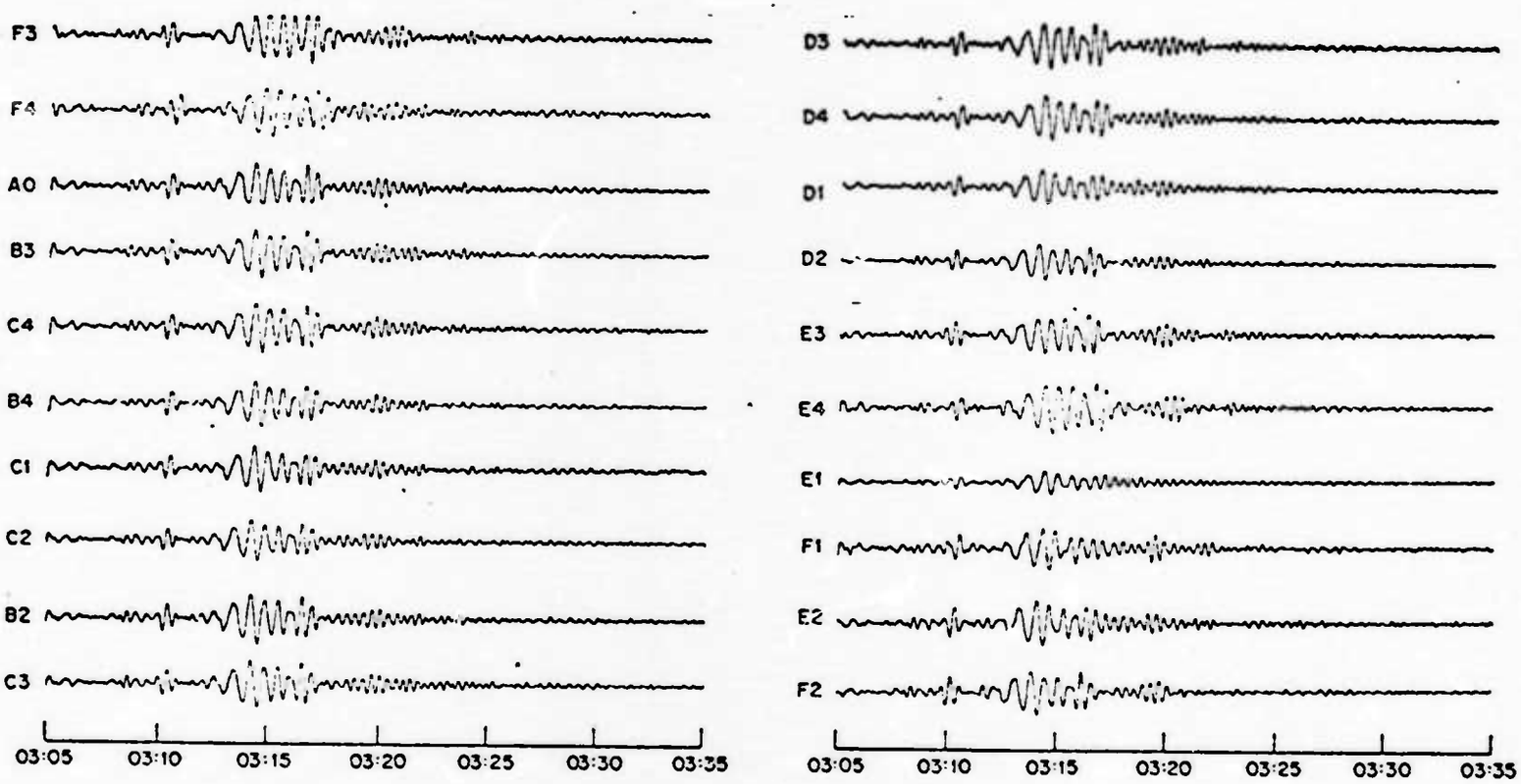

Fig. 10: The Long-Period Wave Forms for Event 3, the March 2, 1967, Ecuador Event. From Capon and Evernden (1971)

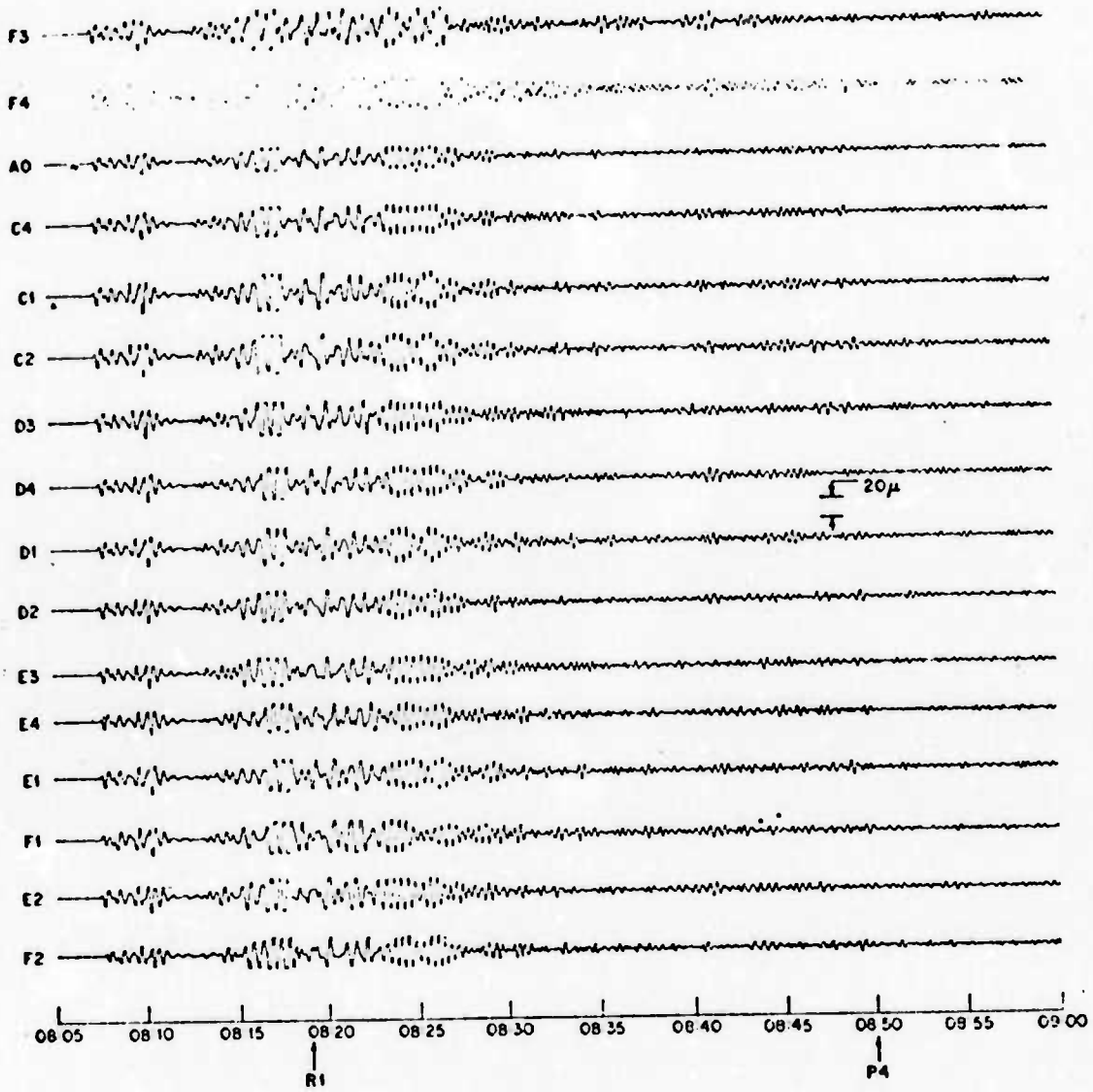

Fig. 11: The Long-Period Wave Forms for Event 19, the October 15, 1967, Event near the Coast of Nicaragua. From Capon and Evernden (1971)

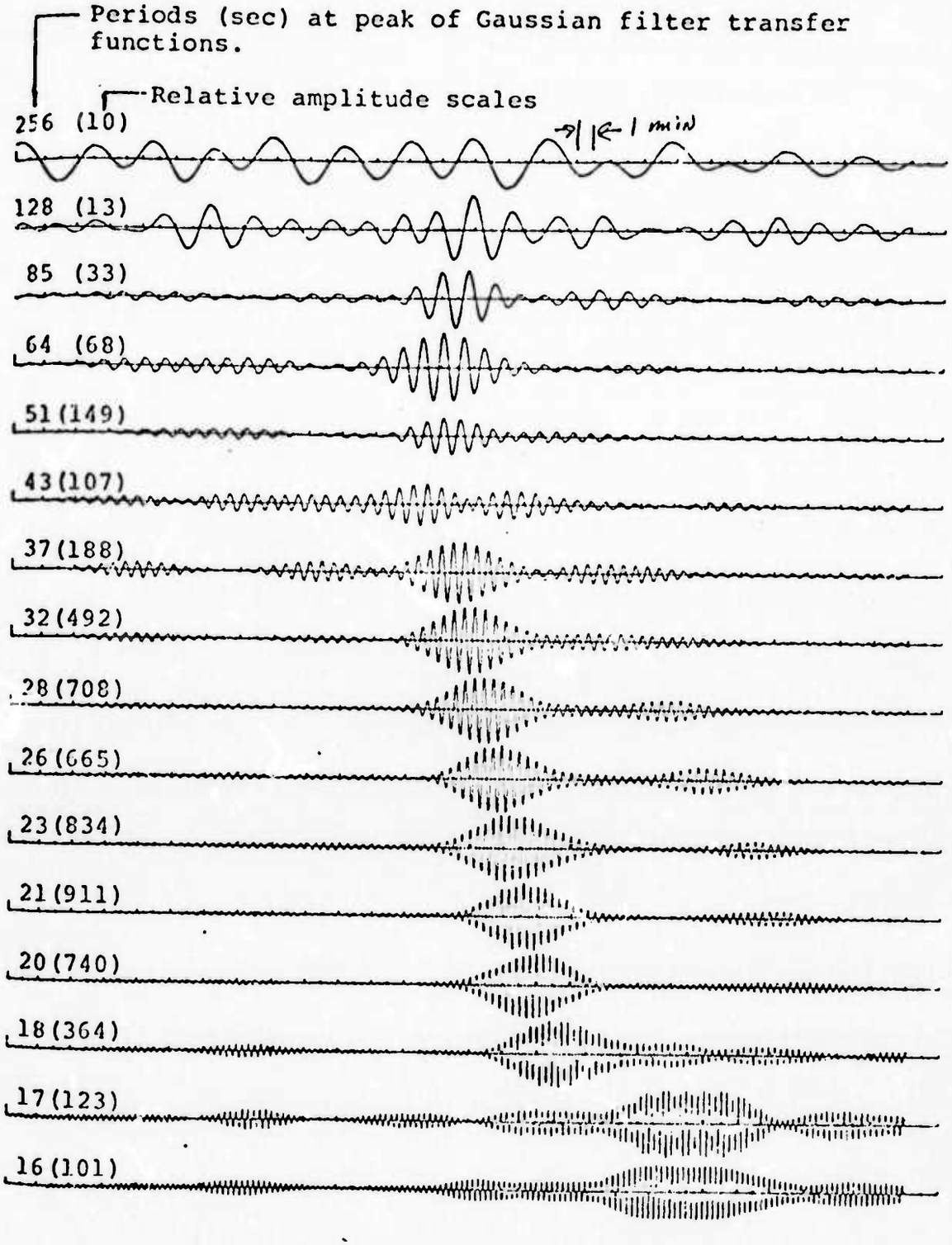

Fig. 12: Narrow-bandpass Filter Traces of the Vertical Component, Mid-Atlantic Ridge Earthquake. From Newton, 1973.

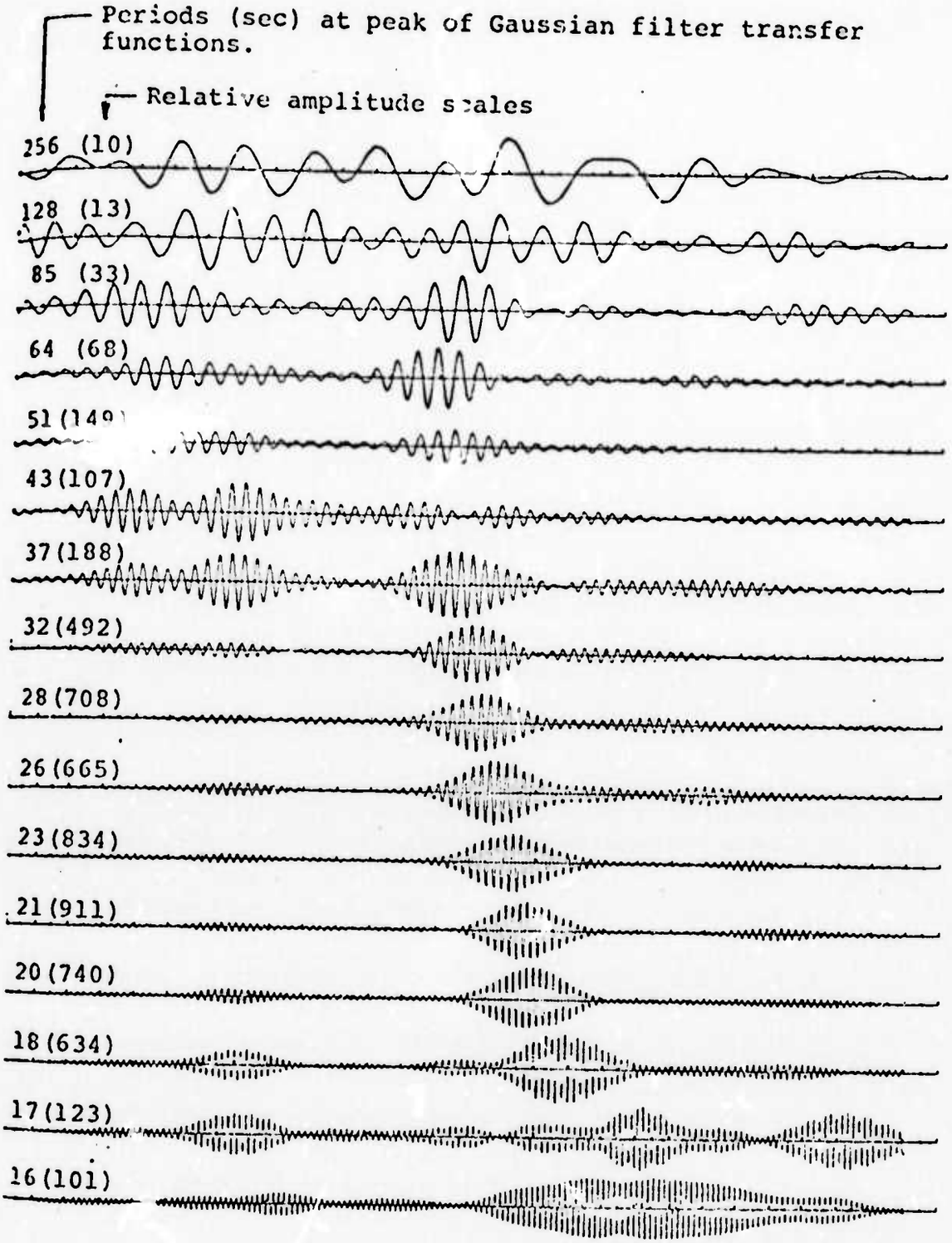

Fig. 13: Narrow-bandpass Filter Traces of the Radial Component Seismogram Containing the Fundamental Mode Rayleigh Wave from the Mid-Atlantic Ridge Earthquake.

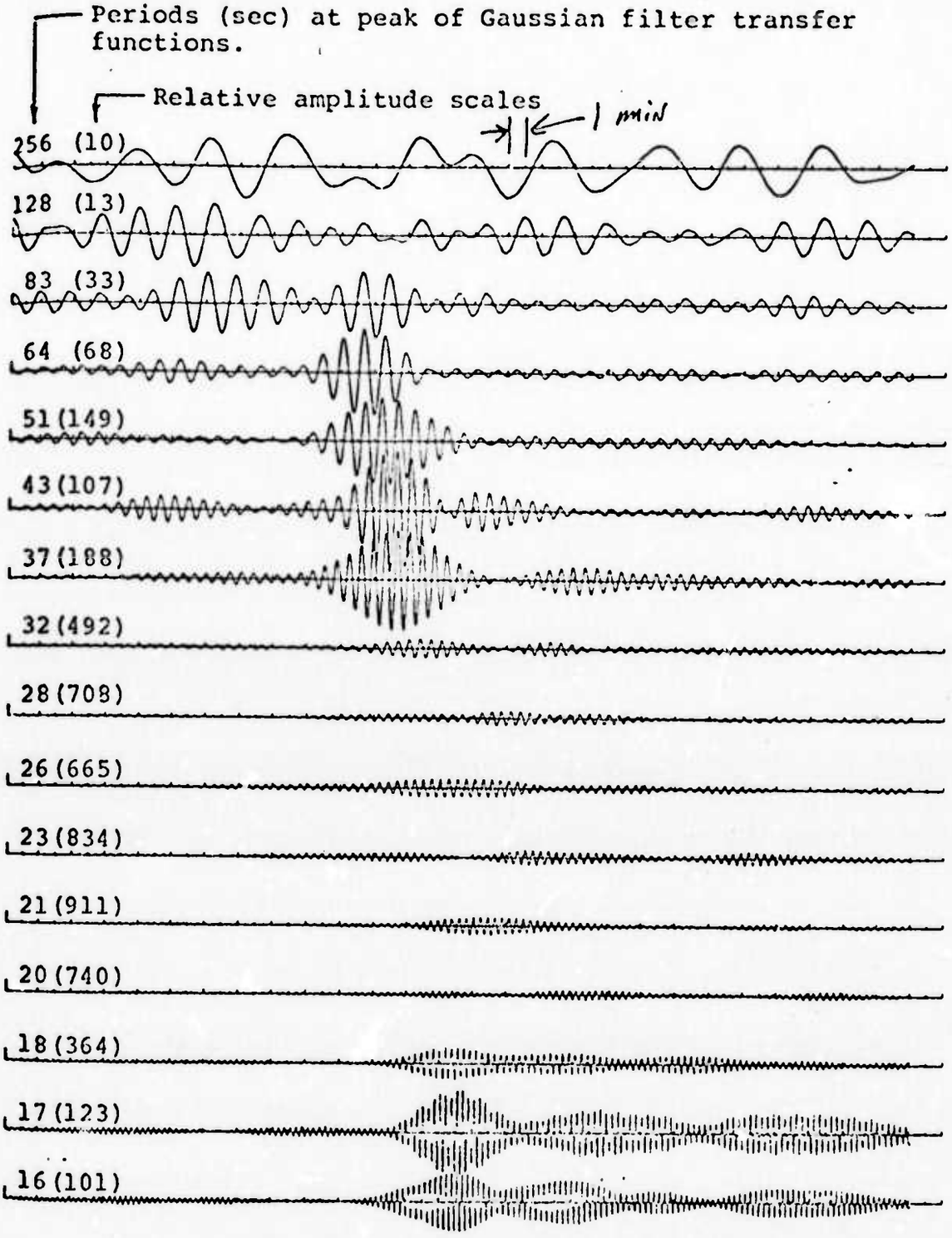

Fig. 14: Narrow-bandpass Filter Traces of the Transverse Component Seismogram Containing the Fundamental Mode Rayleigh Wave from the Mid-Atlantic Ridge Earthquake.

spectral estimates used for the high rssolution f-k analysis. This occurs because the 20 second power level is much above the 40 second power on the LASA seismometer outputs. To eliminate this problem, Capon and Evernden (1971) used a low pass Chebyshev filter. (See Figure 8). The spectral leakage problem will probabl, not be a problem with our high gain, longer period seismometers.

3.2 On the Ellipticity Filter

Newton (1973) (copy of appendix enclosed) tried a method of determining the arrival azimuth based on the assumption of a 90^{o} phase shift between the radial and vertical signals. The method was to find the direction at which the phase shift was 90^{o}. The method worked for simulated data. However, it did not do well on real signals. Newton attributed the failure to an extreme sensitivity to the 90^{o} phase shift assumption. He points out that, if the ellipticity is changing with frequency, the "ellipticity" of a finit bandwidth signal will not have a 90^{o} phase shift. He also did an experiment in which artificial data was used. When the radial data was delayed by one second, the phase shifts which resulted led to large errors in the azimuth determined by the algorithm.

The difficulty Newton had in getting the azimuth for a single Rayleigh wave may indicate that we will have difficulty in the case of the arrival of two Rayleigh waves. If we do have difficulties, one thing that may help is to assume that the explosion signal is coming along the great circle direction. (This assumption is valid for most events at 40 second periods and longer; this was discussed in a previous section of this report) The five other quantities (complex amplitudes of the two signals and azimuth of interfering events) could be found by least squares. This procedure would perhaps be more robust than the solution for all 6 quantities. This approach is supported by

Newton (p. 93); he states that the most correct estimate of the radial power was obtained by using the great circle azimuth.

It appears that multiple reflected P and S body waves will also cause difficulty. It may be worth while to consider the effect of these waves on the filter.

4.0 General Comment

I believe that there are limits to the signal - to interference gain - we can get with a single seismometer. In the course of our work on the single seismometer processing, I believe we should assemble data on signal properties and the three-component coherencies of signals. If we can, we should consider processing methods for small arrays, with perhaps 4 high gain, 3-component seismometers. If the 40 second band pass is useful, then I am sure arrays will eventually be used.

I think that 40 second periods may be of great use in source estimation. This is because lateral refractions are not important at this frequency. Thus, geometrical spreading and focusing (McGarr, 1969; McGarr, 1972; Aki et al. 1972) which is so severe at 20 second period will not be as important at 40 seconds. Therefore, amplitude estimates at 40 seconds should be more reliable.

I have some information at hand on explosion spectra but have not included it at this time.

Appendix

(From Newton 1973)

Appendix E

NULL METHOD FOR DETERMINING RAYLEIGH WAVE PROPAGATION DIRECTIONS

The fundamental and higher modes of Rayleigh waves are characterized by the elliptical particle motion where the vertical and horizontal components have a constant phase difference of $\pi/2$. If the motion is retrograde the radial phase leads and for prograde motion the vertical phase leads, and the transition from one to the other occurs at a node of either of the components.

If $w(t)$ denotes a vertical component seismogram then the analytical signal is the complex representation of $w(t)$, defined by $S(t) = w(t) - i\hat{w}(t)$, where $\hat{w}(t)$ is the Hilbert transform of $w(t)$. $\hat{w}(t)$ is referred to as the "quadrature" signal and $w(t)$ as the "cophase" signal, (see Bracewell, 1965). The cophase and quadrature signals are also characterized by a $\pi/2$ phase difference, and the quadrature phase leads.

Now consider the horizontal component seismograms h_1 and h_2, which are recorded by the orthogonally oriented instruments. If θ' is the angle between the installed azimuth for h_1 and the propagation direction, θ_o, for a Rayleigh wave, then the radial, $u(t)$, and transverse, $v(t)$, seismograms are

$$\begin{bmatrix} u \\ v \end{bmatrix} = \begin{bmatrix} \cos\theta' & \sin\theta' \\ -\sin\theta' & \cos\theta' \end{bmatrix} \cdot \begin{bmatrix} h_1 \\ h_2 \end{bmatrix}.$$

Assuming that only Rayleigh motion is present on u and w then

$$\frac{u-i\hat{u}}{w-i\hat{w}} = \frac{U}{W} = \left|\frac{U}{W}\right| e^{i(\phi_u-\phi_w)} = \left|\frac{U}{W}\right| e^{\pm i\pi/2} = \pm i\left|\frac{U}{W}\right| .$$

Therefore

$$\text{Real}\left\{\frac{u-i\hat{u}}{w-i\hat{w}}\right\} = \frac{uw+\hat{u}\hat{w}}{w^2+\hat{w}^2} = 0$$

which gives the null relation

$$uw+\hat{u}\hat{w} = 0.$$

Making the substitutions

$$u = h_1 \cos\theta' + h_2 \sin\theta'$$

and

$$\hat{u} = \hat{h}_1 \cos\theta' + \hat{h}_2 \sin\theta',$$

we can solve for θ':

$$\theta' = -\tan^{-1}\left[\frac{(\hat{h}_1\hat{w}+h_1 w)}{(\hat{h}_2\hat{w}+h_2 w)}\right] .$$

This algorithm was tested using synthetic signals, the radial component having the same spectrum and group delays as the vertical but a constant phase difference of $\pi/2$, and the transverse component was sinusoidal with slowly changing period and with maximum amplitude approximately the same as the other components. Except for the leading and trailing edges of the Rayleigh wave window the computed θ' was zero.

When the vertical component was shifted by one second with respect to the horizontal components θ' was seldom zero and only for a short window where the signal amplitude was the largest did θ' usually fall within 10 degrees of zero. This means that digitized seismograms must have nearly perfect synchronization between components, i.e., instrument group delays must be uniform and sampling must be synchronous.

Another pitfall for this algorithm occurs when the ellipticity is changing. This effect can be seen graphically by drawing two vectors having a given amplitude ratio and phase separation and then drawing two vectors with phases $\pi/2$ greater than the first two and with a different amplitude ratio. Although the $\pi/2$ phase difference exists between the pairs, it does not exist between the resultant vectors. It was thought that this problem should vanish when band filtering is used because the ellipticities for realistic earth structures are slowly varying with frequency. However, the complete failure for the method when applied to high signal-to-noise seismograms prompted a test of this assumption.

Using the cophase and quadrature signals of a vertical component seismogram as the vertical and radial test signal components, it was found that $uw + \hat{u}\hat{w}$ did indeed vanish. When broad-band Gaussian-shaped filters were applied to the two components using slightly different center frequencies, $uw + \hat{u}\hat{w}$ did not vanish. It was concluded that slight departures from a $\pi/2$ phase difference between components, such

as would appear with even small amounts of noise and when the ellipticity is frequency dependent, are sufficient to render useless the null method for determining Rayleigh wave propagation directions.

REFERENCES

Note: All these references are not used in the text but are relevant.

1. Aki, K., Mendihuren, J.A., and Tsai, Y.: "Reply," J. Geophys. Res., 77: 3827-3830, 1972.

2. Canitez, N. and Toksoz, M.N.: "Focal Mechanism at Source Depth of Earthquakes from Body and Surface Wave Data," BSSA, 61: 1369-1379, 1971.

3. Capon, J.: "Analysis of Rayleigh-Wave Multipath Propagation at LASA," BSSA, 60: 1701-1732, 1970.

4. Capon, J.: "Investigation of Long-Period Noise at the Large Aperture Seismic Array," J. Geophys. Res., 74: 3182-3194, 1969.

5. Capon, J.: "Analysis of Microseismic Noise at LASA, NOSAR and ALPA," Geophys. J., 35: 39-54, 1973.

6. Capon, J.: "Comparison of Love and Rayleigh Wave Multipath Propagation at LASA," BSSA, 61: 1327-1344, 1971.

7. Capon, J. and Evernden, J.F.: "Detection of Interfering Rayleigh Waves at LASA," BSSA, 61: 807-850, 1971.

8. Derr, J.S.: "Discrimination of Earthquakes and Explosions by the Rayleigh-Wave Spectral Ratio," BSSA, 60: 1653-1668, 1970.

9. Douse, E.J. and Sorrells, G.G.: "Prediction of Pressure Generated Earth Motion Using Optimum Filters," Teledyne, Inc., Technical Report 74-6, Geotech Division, Garland, Texas, August 1, 1974.

10. Douglas, A. et al.: "The Analysis of Surface Wave Spectra Using a Reciprocity Theorem for Surface Waves," Geophys. J. of R. Astr. Soc., 23: 207-223, 1971.

11. Larson, R.J. et al.: "Correlation of Winds or Geographic Features with Production of Certain Infrasonic Signals in the Atmosphere," Geophys, J., 26: 210-214, 1971.

12. Marshall, P.D.: "Aspects of the Spectral Differences Between Earthquakes and Underground Explosions," Geophys. J.R. Ast. Soc., 20: 397-416, 1970.

13. McGarr, A.: "Comments on Some Papers Concerning Amplitudes of Seismic Surface Waves," J. Geophys. Res., 77: 3823-3826, 1972.

14. McGarr, A.: "Amplitude Variations of Rayleigh Waves, Horizontal Refraction," Bull. Seis. Soc. Am., 59: 1307-1334, 1969.

15. Savino, J.M., McCamy, K., and Hide, G.: "Structures in Earth Noise Beyond Twenty Seconds - A Window for Earthquakes," BSSA, 62: 171-176, 1972b.

16. Savino, J.M., Murphy, A.J., Ryan, J.M.W., Tatham, R., Sykes, L.R., Choy, G.L., and McCamy, K.: "Results from High-Gain, Long Period Seismograph Experiments," Geophys. J.R. Astr. Soc., 31: 179-203, 1972a.

17. Sorrells, G.G., McDonald, J.A., Dev, Z.A., and Herrin, E.: "Earth Motion Caused by Local Atmospheric Pressure Changes," Geophys. J., 26, 1971.

18. Sorrells, G.G. and Douse, E.J.: "Studies of Long-Period Noise Generated by Atmospheric Pressure Changes," Teledyne, Inc., Technical Report 74-5, Geotech Division, Garland, Texas, August 1, 1974.

19. Sorrells, G.G. and Goforth, T.T.: "Low Frequency Earth Motion Generated by Slow-Propagating, Partially Organized Pressure Fields," Bull. Seis. Soc. Am., 63: 1583-1601, 1973.

20. Sorrells, G.G.: "A Preliminary Investigation into the Relationship between Long Period Seismic Noise and Local Fluctuations in the Atmospheric Pressure Field," Geophys. J., 26: 71-82, 1973.

21. Ziolkowski, A.: "Prediction and Suppression of Long-Period, Non-Propagating Seismic Noise," Bull. Seis. Soc. Am., 63: 937-958, 1973.